Investigation of Soil Nailing Systems

S. BANG, C. K. SHEN, J. KIM, AND P. KROETCH

Benefits of using the soil nailing system in reinforcing slopes and excavations have been widely known among geotechnical engineers and proven very effective. The soil nailing system essentially modifies the strength characteristics of weaker soil adjacent to slopes and excavations, thereby allowing safe construction without endangering stability. An analytical formulation for the design of a soil nailing system based on two-dimensional plane strain limiting equilibrium is presented. Various design parameters such as soil type, depth of excavation, geometry of the nails, spacing of the nails, variation of ground surface, layered soil profile, inclined panel facing wall, and various loading conditions are included. An analytical parametric study to identify the effects of several pertinent parameters on the overall factor of safety of the soil nailing system has also been conducted and the results are included.

An in situ lateral earth support system, known as the soil nailing system, has been introduced and widely adopted in practice in recent years and summarized by Mitchell (*1*). In this technique, the native soil adjacent to the slope or excavation is strengthened by a series of grouted anchors so that it can remain stable at depths that would normally require the installation of a lateral support system. This method requires no pile driving; therefore, it produces less noise and vibration during construction than typical conventional lateral support systems. The details of the soil nailing system as well as its advantages over conventional lateral earth support systems are described elsewhere (*1–3*).

An extensive study of the soil nailing system including the design and analysis methods have been conducted by the writers and published elsewhere (*4–6*). However, the original design formulation is limited in its applicability, since it only considers a vertical cut on a level ground surface with constant nail length. This study expands the original formulation by including random ground surface geometry, variable nail length, multiple layered soil profile, various loading conditions, and inclined panel facing wall. In addition, the factor of safety is calculated by comparing the components of total resisting force and total driving force along the direction of driving force. Details of the analytical formulation are explained, and effects of several parameters on the overall stability of the soil nailing system are discussed.

BACKGROUND

Several design methods have been developed during the last two decades. These design procedures involve different definitions of factor of safety and various assumptions regarding the failure mechanism, the types of soil-reinforcement interaction, and the resisting force calculation in the reinforcing nails. A good summary is provided by Juran et al. (*7*).

All the available design methods can be divided into two general groups: the local stability approach and the global stability approach.

The first approach is based on the analysis of the local equilibrium condition of the active zone, which is bounded by the assumed failure surface. Assumptions involved in this approach are that the failure is caused by a progressive breakage or slippage of the reinforcing nails and that, at failure, the shear strength of the soil is fully mobilized along the entire assumed failure surface. Solution of this approach involves determining the locus and the values of maximum tensile force, shear force, and bending moment in each reinforcing nail (*7*). An example of this is a kinematic limit design method of soil nailing systems recently developed by Juran et al. (*7*). This method is intended to estimate the local stability of the soil mass near the nail.

The second approach is based on the consideration of the nailed soil structure and its surroundings. A classical slope stability analysis method is usually adopted to evaluate the factor of safety with respect to the global failure (i.e., sliding, overturning, etc.) by taking into consideration the tensile, shearing, and pullout resistance of the reinforcing nails crossing the assumed failure surface.

Many methods are currently available for the design of soil nailing systems [e.g., methods developed by Gässler and Gudehus (*8*), Schlosser (*2*), Shen et al. (*1*), etc.]. Most of them are based on limiting equilibrium analysis. However, definitions of factor of safety, failure mechanism, soil-reinforcement interaction, and resisting forces provided by reinforcing nails in each of the methods are not the same.

The limiting equilibrium analysis is best suited for analyzing the global stability instead of the local stability of individual components of the soil nailing system. Therefore, the use of limiting equilibrium analysis for the determination of nail dimensions may not yield reliable results.

LIMITING EQUILIBRIUM FORMULATION

The proposed limiting equilibrium approach is based on the assumption that the failure surface can be represented by a parabolic curve passing through the toe of the wall. This assumption has been derived from the results of finite element study of in situ reinforced soil (*4*). The potential failure surface identified from the finite element study passes more or less through the toe of the wall and forms a curved surface as it propagates upward. Centrifuge model study has also been performed to validate this assumption (*6*). A classical method

S. Bang, J. Kim, and P. Kroetch, South Dakota School of Mines and Technology, 501 E. St. Joseph, Rapid City, S.Dak. 57701. C. K. Shen, Hong Kong University of Science and Technology.

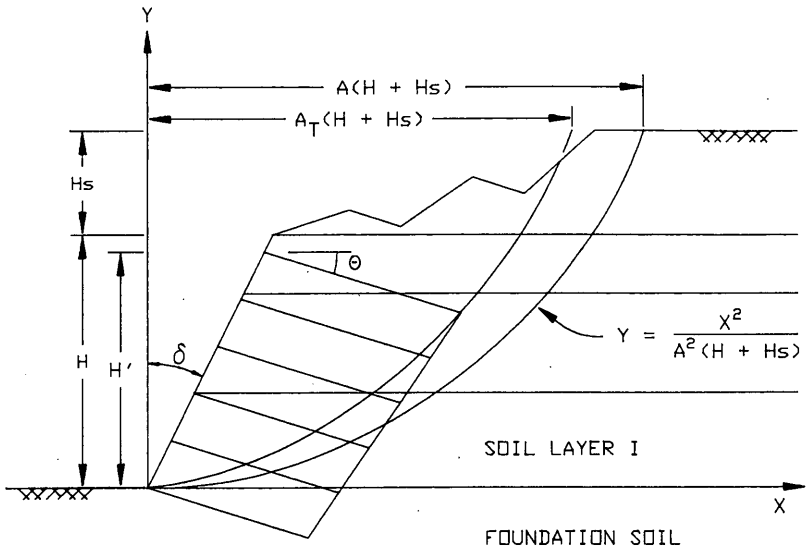

FIGURE 1 Assumed potential failure surface.

of equilibrium analysis is then used to evaluate the stability of the soil nailing system by considering the contribution of the nails to overall stability. The tensile forces developed in the reinforcing nails are divided into tangential and normal components along the failure plane. These force components are then included in the force equilibrium equations. The maximum tensile stress in each reinforcing nail is calculated and compared with the tensile strength of the nails to identify the possibility of nail yielding. The overall minimum factor of safety is then obtained by considering a series of failure surfaces.

Figure 1 shows the assumed potential failure surface and geometric parameters associated with it. The point at which the parabola intersects the ground surface is determined by the value A. Term A_T describes the parabola that intersects the end of the uppermost nail. In this formulation, it is assumed that soil layers are horizontal and the nails are inclined at the same angle.

Figure 2 shows a free body diagram in which the failure surface extends beyond the reinforced soil zone. The tangential forces S_2 and S_3 developed along the potential failure surface are assumed to be parallel to the corresponding chords.

The equilibrium equations of Element 1 (reinforced soil zone) yield the following:

$$N_2 = (W_1 - S_1)\cos \alpha_3 - (N_1 + k_h W_1)\sin \alpha_3 \quad (1)$$

$$S_2 = (W_1 - S_1)\sin \alpha_3 + (N_1 + k_h W_1)\cos \alpha_3 \quad (2)$$

where

W_1 = weight of Element 1,
S_1 = tangential force between Elements 1 and 2,
α_3 = inclination angle of Force S_2, and
k_h = horizontal body force coefficient.

The equilibrium equations of Element 2 produce

$$N_3 = (W_2 + S_1)\cos \alpha_5 + (N_1 - k_h W_2)\sin \alpha_5 \quad (3)$$

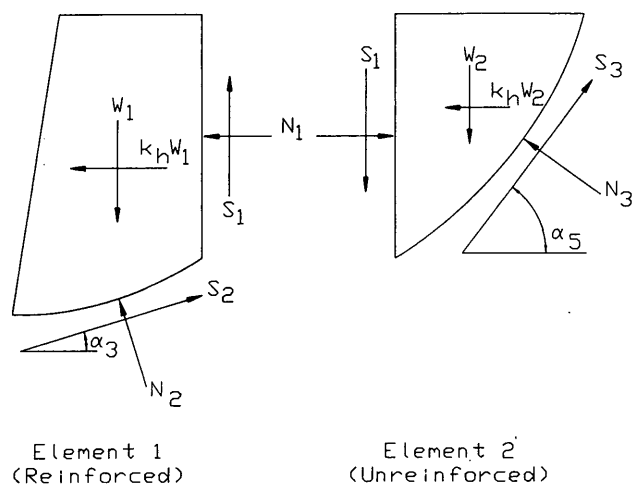

FIGURE 2 Free body diagram.

$$S_3 = (W_2 + S_1)\sin \alpha_5 - (N_1 - k_h W_2)\cos \alpha_5 \quad (4)$$

where W_2 is the weight of Element 2 and α_5 is the inclination angle of Force S_3.

Elements 1 and 2 may have different factors of safety because of different inclination angles of the potential failure surface at the base of each element. To overcome this discrepancy, the following steps have been taken to estimate the overall factor of safety. First, the total driving force, S_D, is found by adding the individual element driving forces vectorially considering the directions of the forces.

$$S_D = \sqrt{S_{DX}^2 + S_{DY}^2} \quad (5)$$

$$\tan \alpha_D = S_{DY}/S_{DX} \quad (6)$$

where

$S_{DX} = S_2\cos \alpha_3 + S_3\cos \alpha_5$
$S_{DY} = S_2 \sin \alpha_3 + S_3\sin \alpha_5$

Next, the total resisting force, S_R, is calculated.

$$S_R = \sqrt{S_{RX}^2 + S_{RY}^2} \tag{7}$$

$$\tan \alpha_R = S_{RY}/S_{RX} \tag{8}$$

where

$S_{RX} = (c_1' L_3 + T_T + N_2' \tan \phi_1')\cos \alpha_3 + (c_2' L_2' + N_3 \tan \phi_2')\cos \alpha_5$,
$S_{RY} = (c_1' L_3 + T_T + N_2' \tan \phi_1')\sin \alpha_3 + (c_2' L_2' + N_3 \tan \phi_2')\sin \alpha_5$,
c_1' = developed cohesion for Element 1 = c_1/FS_c,
c_2' = developed cohesion for Element 2 = c_2/FS_c,
FS_c = factor of safety with respect to cohesion,
ϕ_1' = developed friction angle for Element 1 = $\tan^{-1}(\tan \phi_1/FS_\phi)$,
FS_ϕ = factor of safety with respect to friction,
ϕ_2' = developed friction angle for Element 2 = $\tan^{-1}(\tan \phi_2/FS_\phi)$,
$N_2' = N_2 + T_N$,
$T_N = \Sigma T_i \cos(90° - \alpha_3 - \Theta)$,
ΣT_i = resultant of the axial forces in the portion of the reinforcing nails beyond the assumed failure surface,
$T_T = \Sigma T_i \sin(90° - \alpha_3 - \Theta)$, and
L_2 = length of the entire failure arc.

Finally, the global factor of safety is calculated by comparing the component of the total resisting force along the direction of driving force with the magnitude of total driving force, that is,

$$FS = \frac{S_R \cos(\alpha_R - \alpha_D)}{S_D} \tag{9}$$

It is assumed that at any given time equal percentages of soil cohesion and friction are mobilized. Therefore, the desired global factor of safety is obtained by equating those factors of safety, that is,

$$FS_c = FS_\phi = FS \tag{10}$$

Iteration is performed to obtain the global factor of safety.

In Equations 7 and 8, c_1', c_2', ϕ_1', and ϕ_2' are the soil strength parameters of homogeneous soil. It is therefore necessary to modify these values when multiple soil layers exist. Weighted average values have been used for this purpose:

$$c' = \sum c_i' L_i/L_A \tag{11}$$

$$\tan \phi_1' = \sum_{\text{Element 1}} \tan \phi_i' L_{ai}/L_1 \tag{12}$$

$$\tan \phi_2' = \sum_{\text{Element 2}} \tan \phi_i' L_{ai}/L_2 \tag{13}$$

where

c_i' = developed cohesion of ith soil layer,
L_{ai} = length of arc of ith soil layer,
ϕ_i' = developed friction angle of ith soil layer,
L_A = entire length of failure surface arc,
L_1 = length of failure surface arc of Element 1, and
L_2 = length of failure surface arc of Element 2.

The original formulation (*1*) is restricted to the case of a vertical cut on a level ground surface with constant nail length and homogeneous soil profile. Surface loading conditions other than the ground surcharge are not considered. Expansion of the original formulation, considering the variation of several additional parameters, is described below.

Two cases are considered separately: Case 1 with a failure surface extending beyond the reinforced zone and Case 2 with a failure surface lying entirely within the reinforced soil zone. Note that the effect of layered soil profile is included in the formulation by considering the discrete geometry of each soil layer and its material properties.

Case 1 ($A \geq A_T$)

In Figure 2, α_3 is the direction of the tangential force acting along the bottom of Element 1 and is assumed to be parallel to the corresponding chord. That is,

$$\alpha_3 = \tan^{-1}\left(\frac{Y_c}{L_T \cos \Theta + H' \tan \delta}\right) \tag{14}$$

where

Y_c = vertical distance of the portion of a potential failure surface inside the reinforced soil zone,
$H' = H - VS_1$,
H = height of the wall, and
VS_1 = vertical distance from the top of wall to the uppermost nail.

Also in Figure 2, α_5 is the direction of tangential force acting along the bottom of Element 2 and is also assumed to be parallel to the corresponding chord. It is expressed for a typical case as

$$\alpha_5 = \tan^{-1}\left(\frac{H + H_s - Y_c}{A(H + H_s) - L_T \cos \Theta - H' \tan \delta}\right) \tag{15}$$

where H_s is the thickness of ground surface above the wall.

W_1 is the weight of reinforced soil zone (Element 1) including the soil mass above the top of the wall. W_1 therefore may consist of multiple layers of soil with different unit weights. Thus it is the sum of the weights of all layers within the Element 1 (W_i). In a typical case, it is expressed as

$$W_i = \int_{H_i}^{H_{i+1}} \tau_{i+1} A\sqrt{y(H + H_s)}\, dy - \tau_{i+1}(H_{i+1}^2 - H_i^2) \tan \delta/2 \tag{16}$$

where τ_i is the unit weight of the ith soil layer.

Similarly, W_2 can be calculated from the sum of

$$W_i = \int_{H_i}^{H_{i+1}} \tau_{i+1} A\sqrt{y(H + H_s)}\, dy - \tau_{i+1}(L_T \cos \Theta + H' \tan \delta)(H_{i+1} - H_i) \tag{17}$$

N_1 is the resultant of lateral earth pressure developed between Elements 1 and 2. In the case of a homogeneous soil

layer of height H, N_1 is expressed as

$$N_1 = K\tau(H - Y_c)^2/2 \quad (18)$$

where K is the lateral earth pressure coefficient.

At-rest lateral earth pressure coefficient, K_o, has been used to describe the force N_1.

For a multiple layered soil profile, soil layers that lie above the layer in question are represented by an equivalent surcharge load in calculating the resultant force. Term N_1 is therefore the sum of the resultant forces from each layer:

$$N_1 = \sum N_i \quad (19)$$

where N_i is the resultant of the ith layer.

Case 2 ($A < A_T$)

The difference between Cases 1 and 2 is the expression of x-directional coordinate of the interface of Elements 1 and 2. In Case 1, the x-coordinate of the interface of Elements 1 and 2 is ($L_T \cos \Theta + H' \tan \delta$), which is the x-coordinate of the end of the uppermost nail. But in Case 2, the interface lies at the intersection between the failure surface and the uppermost nail. The x-coordinate of the intersection between the failure surface and the upper most nail, X_c, is expressed as

$$X_c = {}^1/_2\left[-A^2 (H + H_s)\tan \Theta + \sqrt{A^4(H + H_s)^2 \tan^2\Theta + 4A^2(H + H_s)H'(1 + \tan\delta \tan\Theta)}\right] \quad (20)$$

Therefore, if ($L_T\cos \Theta + H'\tan \delta$) is replaced by X_c in the solution of Case 1, the solution of Case 2 is obtained.

Calculation of Tensile Force in Nails

In this formulation, the developed nail force can be calculated in two ways. One approach assumes that the nail force is proportional to the overburden. However, because of possible soil arching, especially in dense cohesionless soils, the developed forces within the same length nails may remain more or less constant beyond a certain depth. For this reason, the analysis method allows an alternative method of estimating the nail axial force (i.e., by specifying the axial force per unit length of the nail). Described below is the calculation of the nail axial force when it is proportional to the depth.

The frictional resistance of each reinforcing nail is expressed as

$$T_i = \pi D L_e (\sigma_n \tan \phi' + c')/\mathrm{HS} \quad (21)$$

where

D = bore hole diameter,
L_e = effective length of the reinforcing nails,
$\tan \phi'$ = developed frictional coefficient,
σ_n = average normal stress,
HS = horizontal spacing of the nails, and
c' = developed cohesion.

From the theory of elasticity,

$$\sigma_n = (\sigma_y \cos^2 \Theta - \sigma_x \sin^2 \Theta)/(\cos 2\Theta + \sin 2\Theta \tan\phi') \quad (22)$$

where

σ_y = overburden acting at the middle of the effective nail length,
$\sigma_x = K\sigma_y$,
Θ = nail inclination angle to the horizontal, and
K = coefficient of lateral earth pressure.

Nail Length

The nail length can be described in several different ways. Two possible descriptions of nail length variation are considered in this formulation: linear variation and step variation. Figure 3 shows how these two descriptions can be applied.

In the case of linear variation of nail length (at depth of d_i), L_i is calculated by Equation 23 for $L_T > L_B$ and by Equation 24 for $L_T < L_B$.

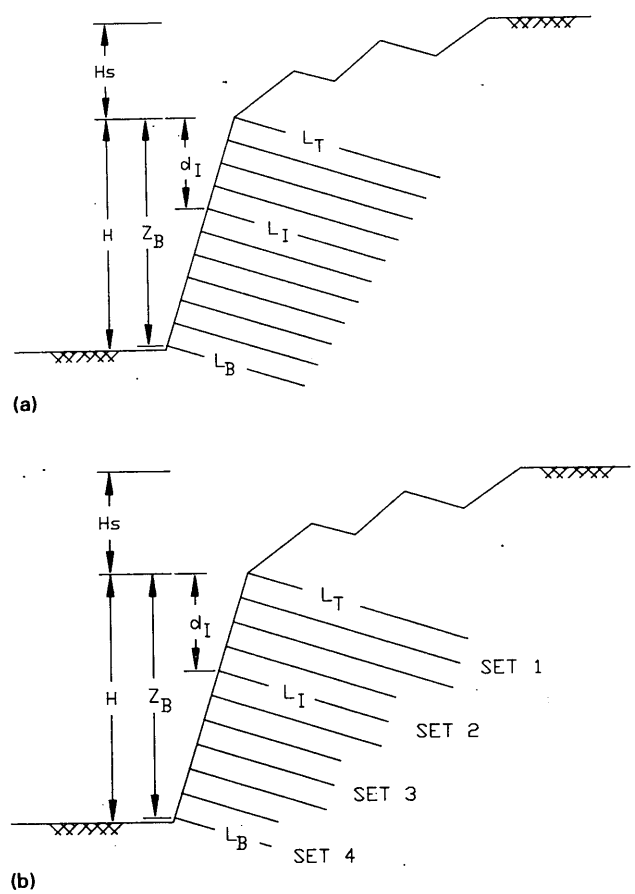

FIGURE 3 Description of nail length: (*a*) linear variation, (*b*) step variation.

$$L_i = (L_T - L_B)(Z_B - d_i)/(Z_B - VS_1) + L_B \quad (23)$$

$$L_i = (L_B - L_T)(d_i - VS_1)/(Z_B - VS_1) + L_T \quad (24)$$

where

L_T = length of the uppermost nail,
L_B = length of the lowermost nail,
Z_B = depth to the lowermost nail from the top of panel facing wall,
VS_1 = depth to the uppermost nail from the top of panel facing wall, and
d_i = depth to ith nail from the top of panel facing wall.

When step variation of nail length is used, the number of nail sets having the same length, the same number of nails in each set, and the nail length in each set are specified as part of the input.

Effective Length

L_e is the effective length of the nail that lies beyond the assumed failure surface.

$$L_e = L_i - [x_i - (H - d_i)\tan\delta]/\cos\Theta \quad (25)$$

where

L_i = length of the nail at depth of d_i,
d_i = depth to ith nail from the top of panel facing wall,
δ = wall inclination angle to the vertical,
Θ = nail inclination angle to the horizontal, and
x_i = x-coordinate of intersection point between the ith nail and failure surface
$= \frac{1}{2}\{-A^2(H + H_s)\tan\Theta + [A^4(H + H_s)^2\tan^2\Theta + 4A^2(H + H_s)(H - d_i)(1 + \tan\Theta\tan\delta)]^{1/2}\}$

Stress σ_y

Term σ_y is the resultant of overburden including the surcharge load acting at the middle length of L_e. Actually, the stress is distributed along the entire effective length whose variation depends on the geometry of the ground surface and the surcharge load. However, σ_y is obtained from the sum of overburden due to all soil layers and equivalent uniform surcharge load:

$$\sigma_y = \sum_{z=0}^{z_i'} \tau_i z_i + q_e \quad (26)$$

where

τ_i = unit weight of ith soil layers,
z_i = thickness of ith soil layers,
q_e = transformed equivalent uniform surcharge load, and
z_i' = distance measured from the ground surface to the center of the contact length of ith nail.

Loading Conditions

It is assumed that the effect of vertical concentrated point loads is the same as increasing the weights of W_1 and W_2 with increase in lateral stress calculated by Boussinesq's equation (*9*) of two-dimensional line load. The distributed surcharge increases the vertical stress as well as the lateral stress as defined by the lateral earth pressure coefficient. The effect of earthquake-induced loading is simulated by a pseudostatic analysis (i.e., by the equivalent horizontal acceleration coefficient).

$$N_2 = (W_1 - S_1)\cos\alpha_3 - (N_1 + k_h W_1)\sin\alpha_3$$

$$S_2 = (W_1 - S_1)\sin\alpha_3 + (N_1 + k_h W_1)\cos\alpha_3$$

$$N_3 = (W_2 + S_1)\cos\alpha_5 + (N_1 - k_h W_2)\sin\alpha_5$$

$$S_3 = (W_2 + S_1)\sin\alpha_5 - (N_1 - k_h W_2)\cos\alpha_5 \quad (27)$$

PARAMETRIC STUDY

The effects of reinforcing nail properties including the spacing, length, and inclination angle on the global stability are briefly discussed below. Also included are the effects of panel facing wall inclination angle, layered soil profile, and pseudostatic earthquake load. Table 1 gives the variations of geometric and material parameters used in the parametric study.

Spacing and Length of Nails

The factor of safety decreases dramatically as the horizontal spacing of nails increases (Figure 4). When the nail length is 20 ft, which is relatively small compared with the height of panel facing wall (50 ft), the factors of safety are much lower than those calculated for longer nails. This is primarily because the contribution of shorter nails to the overall stability

TABLE 1 Geometric and Material Parameters Used

Height of the wall:	50 ft.
Facing wall inclination angle:	0 - 40° (0)
Diameter of the bore hole:	4 in.
Diameter of the nails:	1 in.
Spacing of the nails:	2 - 7 ft. (5)
Length of the nails:	20 - 60 ft. (40)
Yield strength of the nails:	30 - 80 ksi (30)
Inclination angle of the nails:	0 - 40° (15)
Soil unit weight:	100 - 125 pcf (100)
Soil friction angle:	5 - 40° (30)
Soil cohesion:	0.5 - 2 ksf (1)
Earthquake coefficient:	0 - 0.6 (0)
Slope of backfill surface:	0°
Lateral earth pressure coefficient:	1 - sinϕ

Numbers in parentheses are the standard values used in the parametric study.

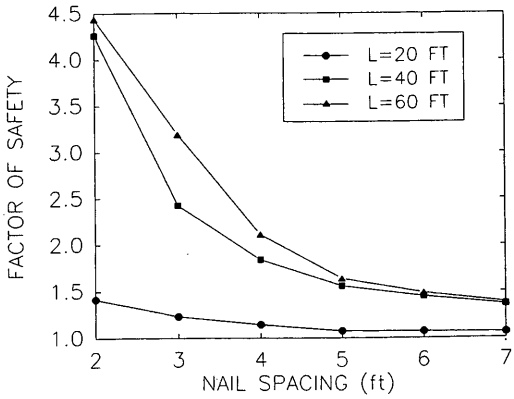

FIGURE 4 Effect of nail spacing.

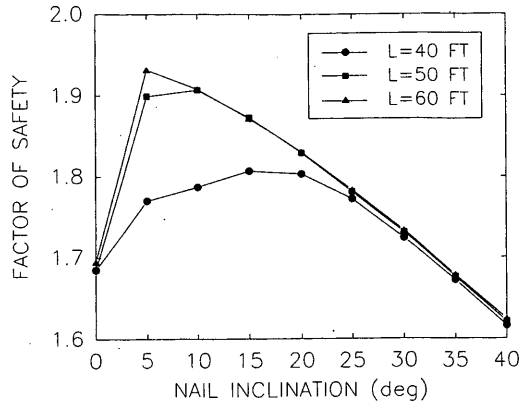

FIGURE 6 Effect of nail inclination angle.

is relatively small. When the nail length is 20 ft, slippage is the dominant failure mechanism, whereas breakage is dominant when the nail lengths are 40 ft and 60 ft. The curves become flatter as the spacing of nails increases because the contribution of nail tensile forces to the global stability again becomes smaller.

Increasing the nail length is equivalent to increasing the contact length between the nails and the surrounding soil. This causes a direct increase in developed nail tensile force. Figure 5 shows the effect of length of reinforcing nails to the overall factor of safety with various spacings of the nails. When the nail length changes from 20 ft to 60 ft, the factor of safety increases by 0.3 to 1.0. Because of the yielding of nails the factor of safety becomes constant with further increases in nail length assuming the cross section and strength of the nails remain the same.

Nail Inclination Angle

The effect of nail inclination angle is shown in Figure 6. The largest factor of safety occurs at a nail inclination angle of approximately 5 to 20 degrees regardless of the nail spacing. This finding confirms the previous result of the optimum nail inclination angle obtained by the writers that was based on simple analytical calculation (*3*).

Inclination Angle of Panel Facing Wall

Increasing the inclination angle of the panel facing wall corresponds to increasing the effective nail length of a given nail and to decreasing the driving forces. Therefore increasing the inclination angle results in increasing the factor of safety. As the panel facing wall inclination angle increases from 0 to 40 degrees, the factor of safety increases almost linearly by approximately 85 percent regardless of the soil strength parameters (Figure 7).

Layered Soil Profile

It is assumed that the developed tensile force is proportional to the overburden, the shear strength of soil, and the contact length between the soil and the nails. Therefore, the tensile stress tends to become larger in nails located near the bottom of the excavation. This indirectly indicates that the stability of the reinforced soil is primarily influenced by the shear strength of the soil layer near the bottom of excavation rather than that near the top if nail force is proportional to the overburden (Figure 8).

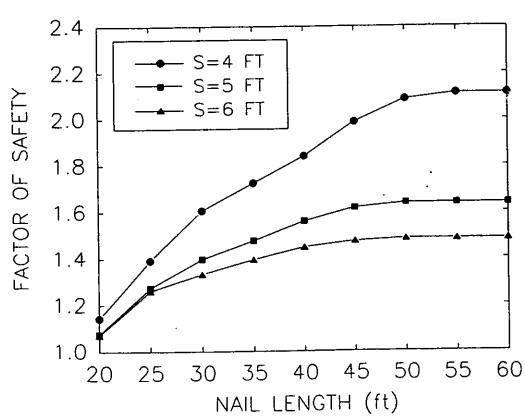

FIGURE 5 Effect of nail length.

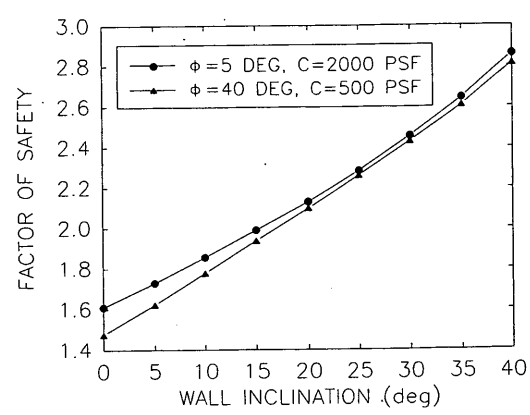

FIGURE 7 Effect of panel facing wall inclination.

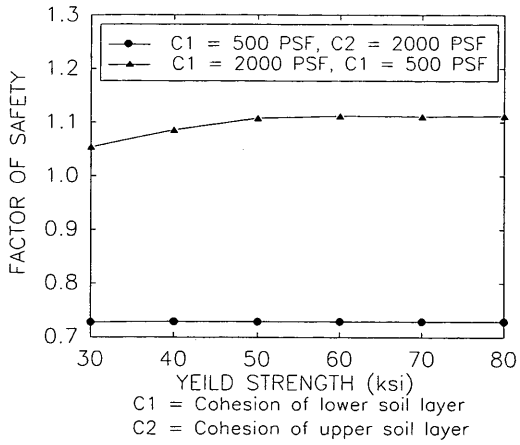

FIGURE 8 Effect of layered soil profile.

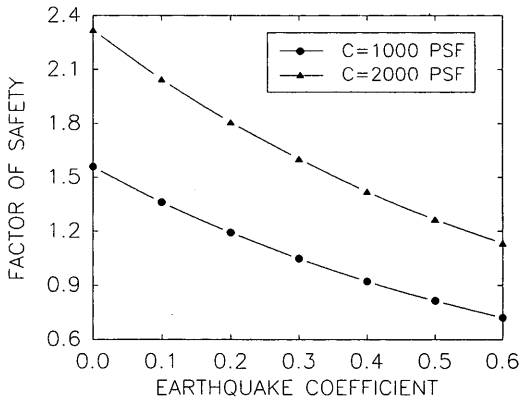

FIGURE 9 Effect of earthquake load.

Earthquake Load

Earthquake loads increase the driving force and reduce the resisting force simultaneously. Therefore the effect of earthquake loads is rather significant (Figure 9). As the horizontal coefficient of acceleration increases from 0 to 0.6, the factor of safety decreases by 50 percent.

CONCLUSIONS

This paper presents the limit equilibrium formulation for the design of a soil nailing system. It expands the original formulation by including the layered soil profile, variable nail length, inclined panel facing wall, random ground surface geometry, ground surcharge, and earthquake loading. The definitions of factor of safety, failure mechanism, and soil-reinforcement interaction remain the same as in the previous formulation. The limiting equilibrium method of analysis is intended to estimate the overall stability of the soil nailing wall against sliding.

A preliminary parametric study to identify the effects of several design parameters on the overall stability has been carried out and the following conclusions have been reached:

1. The nail spacing and length have profound effects on global stability.
2. There is an optimum nail inclination angle, approximately 5 to 20 degrees to the horizontal.
3. The factor of safety is approximately linearly proportional to the inclination angle of the panel facing wall.
4. When the soil is layered, the stability of the soil nailing system is primarily influenced by the soil properties located near the bottom, assuming that the nail axial force is proportional to the overburden.
5. Earthquake loading has a rather significant effect. As the coefficient of horizontal acceleration increases from 0 to 0.6, the factor of safety decreases by as much as 50 percent.

Several recommendations for further study have been identified as a result of this study:

1. The effect of corrosion should be considered for long-term stability analysis.
2. Additional extensive parametric study considering much wider variation is necessary to obtain more detailed quantitative information regarding the effects of design parameters to the global stability of the soil nailing system.
3. The soil-nail interaction behavior needs to be studied in detail so that the correct stress transfer mechanism is modeled in the analysis.
4. The developed analytical formulation and its results need to be verified through detailed experimental scale model or field testing of the soil nailing system.

REFERENCES

1. C. K. Shen, L. R. Herrmann, K. M. Romstad, S. Bang, Y. S. Kim, and J. S. DeNatale. *An In Situ Earth Reinforcement Lateral Support System*. Report 81-03. University of California, Davis, 1981.
2. J. K. Mitchell. *Reinforcement of Earth Slopes and Embankments*. TRB, National Research Council, Washington, D.C., 1987.
3. S. Bang, C. K. Shen, and K. M. Romstad. Analysis of an Earth-Reinforcing System for Deep Excavation. In *Transportation Research Record 749*, TRB, National Research Council, Washington, D.C., 1980.
4. C. K. Shen, S. Bang, and L. R. Herrmann. Ground Movement Analysis of an Earth Support System. *ASCE*, Vol. 107, GT12, Dec. 1981.
5. C. K. Shen, S. Bang, K. M. Romstad, L. Kulchin, and J. S. DeNatale. Field Measurements of an Earth Support System. *ASCE*, Vol. 107, GT12, Dec. 1981.
6. C. K. Shen, Y. S. Kim, S. Bang, and J. F. Mitchell. Centrifuge Modelling of Lateral Earth Support. *ASCE*, Vol. 108, GT9, 1982.
7. I. Juran, G. Baudrand, K. Farrag, and V. Elias. Kinematic Limit Analysis for Design of Soil-Nailed Structures. *Journal of Geotechnical Engineering*, Vol. 116, No. 1, Jan. 1990.
8. G. Gässler and C. Gudehus. Soil Nailing—Some Aspects of a New Technique. *Proc., 10th International Conference on Soil Mechanics and Foundation Engineering*, Vol. 3, Stockholm, Sweden, 1981.
9. B. M. Das. *Principles of Geotechnical Engineering* (2nd ed.). PWS-Kent, 1990.

Publication of this paper sponsored by Committee on Mechanics of Earth Masses and Layered Systems.